

PCCP

Accepted Manuscript



This is an *Accepted Manuscript*, which has been through the Royal Society of Chemistry peer review process and has been accepted for publication.

Accepted Manuscripts are published online shortly after acceptance, before technical editing, formatting and proof reading. Using this free service, authors can make their results available to the community, in citable form, before we publish the edited article. We will replace this *Accepted Manuscript* with the edited and formatted *Advance Article* as soon as it is available.

You can find more information about *Accepted Manuscripts* in the [Information for Authors](#).

Please note that technical editing may introduce minor changes to the text and/or graphics, which may alter content. The journal's standard [Terms & Conditions](#) and the [Ethical guidelines](#) still apply. In no event shall the Royal Society of Chemistry be held responsible for any errors or omissions in this *Accepted Manuscript* or any consequences arising from the use of any information it contains.

ARTICLE

A kinetic and thermochemical database for organic sulfur and oxygen compounds

Cite this: DOI: 10.1039/x0xx00000x

Caleb A. Class^a, Jorge Aguilera-Iparraguirre^{a,b} and William H. Green^{a,*}Received 00th January 2012,
Accepted 00th January 2012

DOI: 10.1039/x0xx00000x

www.rsc.org/

Potential energy surfaces and reaction kinetics were calculated for 40 reactions involving sulfur and oxygen. This includes 11 H₂O addition, 8 H₂S addition, 11 hydrogen abstraction, 7 beta scission, and 3 elementary tautomerization reactions, which are potentially relevant in the combustion and desulfurization of sulfur compounds found in various fuel sources. Geometry optimizations and frequencies were calculated for reactants and transition states using B3LYP/CBSB7, and potential energies were calculated using CBS-QB3 and CCSD(T)-F12a/VTZ-F12. Rate coefficients were calculated using conventional transition state theory, with corrections for internal rotations and tunneling. Additionally, thermochemical parameters were calculated for each of the compounds involved in these reactions. With few exceptions, rate parameters calculated using the two potential energy methods agreed reasonably, with calculated activation energies differing by less than 5 kJ/mol. The computed rate coefficients and thermochemical parameters are expected to be useful for kinetic modeling.

Introduction

Sulfur compounds can be found in almost every aspect of life, and their interactions with oxygenated species play an important role in fuels, geochemistry, and environmental chemistry.^{1, 2} The formation of petroleum in geochemical reservoirs may be accelerated by the presence of weak carbon-sulfur bonds, and the reaction mechanisms of these species can be affected by the presence of water.³⁻⁵

One of the most important sources of sulfur compounds is crude oil, and these compounds will react to form toxic sulfur dioxide if not removed prior to combustion. The desulfurization of crude oil has become a very important topic of study, as sulfur emission standards have tightened and the availability of sulfur-lean feedstock has lessened.⁶ The current industry standard, hydrodesulfurization, requires the use of hydrogen and expensive catalyst to achieve the proper sulfur level, so multiple alternatives are being studied to potentially achieve similar results at a lower cost. Oxidative desulfurization converts thiophenic compounds into more easily removable polar compounds using hydrogen peroxide and a catalyst.⁷ Microbial desulfurization removes sulfur from organic compounds at ambient temperature and pressure.⁸ Treating oil with super-

a) Dept. of Chemical Engineering, Massachusetts Institute of Technology, Cambridge, MA 02139

25 b) Present address: Dept. of Chemistry and Chemical Biology, Harvard University, Cambridge, MA 02138

†Electronic supplementary information (ESI) available. See DOI:

-critical water accomplishes desulfurization without the requirement of any catalyst.⁹ Work in supercritical water upgrading has demonstrated that water generates products with reduced sulfur content and molecular weight.^{10, 11} Water's involvement in this process has been explored via model compound experiments, and investigators have proposed pathways to explain the reactivity of various sulfur compounds in aqueous and supercritical systems.¹² Additional experiments and the advancement of computational chemistry techniques have assisted in the elucidation of this mechanism, showing water to be both a reactant and a hydrogen-transfer catalyst in the mechanism of alkyl sulfide desulfurization.⁹ Based on intermediate studies and quantum chemistry calculations, a plausible pathway for water-aided desulfurization was proposed,⁹ and this is shown schematically in Figure 1. In the proposed mechanism, the water prevents the conversion of the reactive thioaldehyde (reactant **3**) to an oligomer, which is known to occur in the absence of water.¹³ Water participates by adding to the carbon-sulfur double-bond in reaction **c** to form reactant **4**, which readily reacts at high temperature to form hydrogen sulfide, carbon monoxide, and a smaller alkane.

50 Many other pathways are possible, and a full kinetic mechanism of the system based on accurate thermochemical and kinetic data is necessary to evaluate and validate them. Extensive libraries of thermochemical data and reaction rate parameters for hydrogen abstraction, beta scission, and substitution reactions involving organosulfur compounds have been generated by Vandeputte *et al.*¹⁴⁻¹⁶ Rate constants have also been calculated for small-molecule reactions involved in

combustion to form SO_x compounds.^{17, 18} However, these data are not sufficient for accurately modeling the reactions of thiols, sulfides, and thiophenes with oxygenated species. This work focuses on the reactions of sulfur compounds and other species that are likely to be produced in the presence of water at high temperatures. Many of the reactions considered here could also be relevant to organosulfur combustion systems.

Rate parameters in modified Arrhenius form were calculated for 40 reactions that involve organic sulfur and oxygen. These provide rate constants for use in simulations of hydrocarbon mixtures including both sulfur and oxygen, as well as in training sets to develop more general rate estimation rules. Thermochemical parameters, which are required for the calculation of equilibrium constants and temperature changes in reacting systems, have also been computed for each of the species involved in the reactions and compared to the limited data available.

Methods

Thermochemical data were computed using the Gaussian 03 and Molpro quantum chemistry packages.^{19, 20} All species with an even number of electrons were calculated in their singlet state, and radical compounds were calculated in their doublet states. Geometry optimizations and frequency calculations were conducted using B3LYP/CBSB7 in Gaussian 03,^{19, 21, 22} and it was tested that all the reactants and products were indeed minima on the potential energy surface and that all the transition states showed one and only one imaginary frequency that corresponded to the expected reaction coordinate. Multidimensional scans, and additional optimizations when applicable, were also conducted to ensure that the lowest-energy transition state was found for each reaction. These geometries were then used for single point energy calculations at higher levels of theory. Electronic energies were calculated using both the composite CBS-QB3 method^{20, 22, 23} in Gaussian 03 and the explicitly-correlated CCSD(T)-F12a/VTZ-F12 method in Molpro (this will be referred from now on as CCSD(T)-F12).^{20, 24-27}

The slow convergence of CCSD(T) with the basis set size has been known for a long time.^{28, 29} That restricted its application to very small systems.^{30, 31} In the last few years explicitly-correlated methodologies have been introduced to circumvent this problem.^{32, 33} They directly address the fact that conventional coupled-cluster methods approximate wavefunctions based on one-electron basis functions and can hardly describe the electron-electron correlation. This drawback was overcome with the introduction of functions depending explicitly on the inter-electronic distance, as used in the CCSD(T)-F12 family. That makes the basis set convergence much faster and allows us to describe medium-sized systems with basis-set error of less than 1 kcal/mol. These properties have allowed it to be successfully applied in all sorts of fields, including thermochemistry and kinetics.³²⁻³⁶

CBS-QB3 has previously been used in a variety of kinetic studies, including some relevant to sulfur chemistry, and the reaction barriers calculated have been shown to have an

uncertainty of a few kcal/mol.^{22, 23, 37, 38} CBS-QB3 thermochemistry is usually more accurate due to the availability of empirical Bond Additivity Corrections (BAC).³⁹ It appears that CBS-QB3 is becoming obsolete, as new density functionals like M06 and BMK provide comparable accuracy at a much lower cost, and CCSD(T)-F12 methods provide improved accuracy at a still-reasonable cost.^{40, 41} We include CBS-QB3 calculations here nevertheless since a big part of the data available in the literature from the last two decades has been calculated in this way, so a good assessment of its accuracy is still useful.

Partition functions were calculated using the CanTherm software package,⁴² using a scaling factor of 0.99 for the frequency analysis. Enthalpies, entropies, and heat capacities were calculated using CBS-QB3 energies in CanTherm, including the BAC's that are available in literature.³⁹ Preliminary studies on No correction was available for the C=S bond due to the scarcity of experimental data for thiocarbonyl compounds. Calculated parameters were used to generate NASA polynomials for each of the reactants and products. These calculations were used to extend the group additivity scheme for thermochemical properties, which was originally proposed by Benson and Buss, and extended by Vandeputte *et al.* using CBS-QB3 for compounds containing sulfur.^{16, 41, 42}

Using the thermochemical parameters calculated in this work, group additivity values (GAV's) of enthalpy and entropy of formation, and heat capacities between 300 and 1500 K for 15 groups containing both sulfur and oxygen were derived using the regression method discussed by Vandeputte *et al.*¹⁶ Hydrogen Bond Increments (HBI's), as defined by Lay *et al.*,⁴³ were derived for two radical groups including sulfur and oxygen. The values for groups with previously calculated GAV's (i.e. those that do not contain all of sulfur, carbon, and oxygen) were held constant at the literature values.

Transition states were optimized for each elementary reaction, and transition state theory in CanTherm was used to calculate rate coefficients under the ideal gas assumption, correcting for the internal rotations of each single bond within the reactants, products, and transition states. One-dimensional hindered rotations were used in the analysis, optimizing the geometries at the B3LYP/6-311G(2d,p) level at 10-degree increments for each rotatable bond. Asymmetric Eckart tunneling corrections were also calculated, and these corrections were applied to generate the reaction rate constants between 300 and 2000 K.⁴⁴ Rate constants were fitted to the modified Arrhenius form,

$$k(T) = A * T^n * e^{\frac{-E_a}{R*T}}$$

where T is the temperature in Kelvin, R is the gas constant, A and n are fitted constants, and E_a is the fitted activation energy. It is important to note that the fitted E_a is not the same as the reaction energy barrier ΔE_o , the calculated energy difference between the reactants and transition state including zero-point energies (ZPE's). E_a and ΔE_o can differ by multiple kJ/mol. The modified Arrhenius form has been demonstrated to fit rate constants for a variety of organic systems better than the

standard Arrhenius form without the T^n term.^{44, 45} However, due to greater tunnelling effects at lower temperatures, the fitting uncertainty of this form at this limit can exceed a factor of two. Thus, some rate constants were calculated for smaller temperature ranges, and these are noted in the data tables. Care should be taken when extrapolating outside these ranges. These rate parameters were calculated assuming reactant activity coefficients $\alpha_i=1$. The activity for water can vary significantly at supercritical conditions: for example, in the 400 °C and 275 bar experiments of Kida *et al.*,⁹ the activity coefficient of water is calculated to be approximately 0.5[H₂O], reducing the rates by this factor when water is a reactant or collision partner. Thus, the rate parameters in this work should be adjusted to account for the conditions being modeled to avoid introducing additional errors.

Calculation of Rate Constants for Reactions with Submerged Transition States

The reaction barrier was calculated to be significantly negative (i.e. greater than (i.e. greater than the uncertainty of the calculations) for two of the reactions the reactions studied in this work, implying the existence of reactive complexes reactive complexes at lower energy levels than the reactants of the respective the respective reactions. Examples of these reactions are presented in Figure 11 presented in Figure 11 and

Figure 14. The same methods as discussed previously for reactants and products were used to calculate energies and frequencies for the reactive complex of each reaction.

The parameters for each submerged reaction were calculated for the high-pressure limit using CanTherm. The rate k_1 for the formation of complex was assumed to be the collision rate, 10^{13} cm³/(mol*s), and k_{-1} was calculated using thermochemical consistency. The rate of formation of products from the pre-reactive complex, k_2 , was calculated using transition-state theory. The complex is short-lived, so it can be modeled using the quasi-steady-state approximation. The overall rate of product formation for a reaction with two reactants is therefore

$$\frac{dC_P}{dt} = \frac{k_1 k_2}{k_{-1} + k_2} C_{R_1} C_{R_2}$$

and the effective rate constant is

$$k_{eff}(T) = \frac{k_1 k_2}{k_{-1} + k_2}$$

The effective rate constant $k_{eff}(T)$ was calculated at temperatures between 300 and 2000 K, and modified Arrhenius parameters were fit to these calculations to obtain the values reported in the Tables for Reactions 21 and 37. As our primary interest is in supercritical water reactions (with pressures greater than 200 bar), rate constants are reported in the high pressure limit. In some gas-phase situations, the low-pressure limit might be more appropriate than the high-pressure limit values reported here. Even at higher pressures, the collision rate used is a relatively rough estimate, so further refinement of the rate parameters for these two reactions will be necessary if mechanistic model predictions are particularly sensitive to them.

50 Basis Set benchmarking for CCSD(T)-F12 Calculations

Experimental data for the elementary reactions of sulfur compounds is scarce, but a test set of four reactions similar to the types being considered for this work was selected to test the accuracy of CBS-QB3 against CCSD(T)-F12. This includes two hydrogen abstraction reactions,^{46, 47} one radical addition,⁴⁸ and one H₂O elimination reaction.⁴⁹ The first three reactions in this set were previously used to benchmark CBS-QB3 for sulfur chemistry.³⁸ Rate constants were calculated with the previously described methods, and the results are presented in Table 1. Overall, CCSD(T)-F12 calculations outperform those of CBS-QB3. All three basis sets (even double zeta) match the published data within roughly a factor of 2. This suggests that our methods are reasonable for these reaction types, although additional experimental data would be very useful for more substantial benchmarking.

An additional procedure to establish the accuracy of the basis set in the Coupled-Cluster calculations for our particular set of reactions, including both oxygen and sulfur, was defined as follows: in each of the different classes of reactions, the one with the smallest number of electrons was used. These are reactions 1 for the molecular additions of water, 12 for the molecular additions of hydrogen sulfide, 20 for the hydrogen abstractions and 31 for the beta-scissions. The restriction on the size of the reactions allows us to perform calculations on a bigger basis that would it be practical otherwise, and use its results as a benchmark.

We obtained both reactants and transitions states for our set of reactions and performed a consistent set of CCSD(T)-F12a calculations with the basis set series VDZ-F12, VTZ-F12, and VQZ-F12.⁵⁰ CCSD(T)-F12b energies were also calculated with the VQZ-F12 basis set, and these agreed with the F12a energies for the same basis set with an average error of 0.17 kJ/mol.

The convergence with respect to basis set is shown on Table 1. Triple-zeta F12 barrier heights are converged to better than 1 kJ/mol. Double-zeta basis set on the other hand lead to errors above 1 kJ/mol. This is in good agreement with previous studies.⁵¹ In a compromise between accuracy and computational cost, we chose VTZ-F12 basis set as the standard for this study. It is important nevertheless to be aware of the error introduced by such a choice.

While the calculations reported here are converged with respect to basis set, this does not mean they are exact. CCSD(T) is not full-CI, and there are several small neglected terms (Born-Oppenheimer breakdown, relativistic, anharmonicity) which can contribute errors on the order of kJ/mol. Still, we expect that the numbers computed here are rather close to the true energies.

Results and Discussion

Molecular Addition of Water (Hydration of Double Bonds)

Reaction coefficients calculated for the ten reactions involving the molecular addition of water to double bonds, the reverse of which is the elimination of water from an alcohol, are presented in Table 3. These reactions progress via a four-membered ring

transition state. Transition states for reactions 3, 8 and 9 were previously calculated.^{9, 52} All the other geometries were determined in this work and are reported in the Supporting Information. Those geometries were used in this study. Reaction 8 corresponds to the addition of water to the thiocarbonyl group of carbonyl sulfide, while reaction 9 is addition to the carbonyl group. Reactions 10 and 11 are for the addition of water to the carbon-carbon double-bond of thiophene, which also occurs through a four-membered ring transition state. All of these reaction coefficients were calculated using CCSD(T)-F12a//VTZ-F12 energies, with the exception of reaction 6, for which the CBS-QB3 energies were used. A full set of rate parameters calculated for each reaction using CBS-QB3 has also been included in the Supplementary Materials.

The transition state of reaction 1, addition of water to thioformaldehyde, is presented in Figure 2. Calculated reaction parameters for the molecular elimination of water from methanediol and ethanol are available in literature, and using available thermochemistry data we can estimate the activation energy of these reactions in the addition direction.^{53, 54} These are compared with the activation energies of reaction 1 in Table 4. The instability of thiocarbonyl compounds, which are known to polymerize at room temperature, provides for a low-energy pathway for the conversion of this type of compound.¹³ Table 4 shows that the activation energy in both directions is lowest for the thiocarbonyl case, as the 4-center reaction is much more facile for sulfur-containing systems than for C/H/O systems.

Lower A-factors and higher n-factors are calculated with the substitution of a methyl or ethyl group on the thioaldehyde, as in reactions 2 and 3. These reactions have very similar Arrhenius constants, n-factors, and activation energies, and they are predicted to agree within 50% for all temperatures between 300 and 2000 K. This suggests that increasing the length of the thiocarbonyl compound has a minor effect, and will likely have a lesser effect as this chain length increases. Reaction 4 has similar activation energies but a lower A-factor than reactions 1-3 due to the presence of a methyl group on both sides of the thiocarbonyl group, providing a small steric hindrance. The steric effect will increase for addition to branched thioaldehydes, and especially branched thioketones, so these should be explored further when these reactions are of interest.

We compute a barrier height of 144 kcal/mol for the addition of water to benzenethial using CBS-QB3, which is significantly greater than that calculated for addition to an alkyl thioaldehyde, which ranges between 122 and 124 kcal/mol (using CCSD(T)-F12a//VTZ-F12 energies). The transition state geometries for reactions 5 and 6, the addition of water to 2-propenethial and benzenethial, are presented in Figure 3. The lengths of the C-S bonds in the two transition states differ by less than 0.01 Å, and this similarity is reflected in the rate constant calculations. CBS-QB3 calculations on reaction 5 resulted in a reaction barrier of 145 kJ/mol, which is within 1 kJ/mol of the calculated barrier for hydration of benzenethial. As expected, very similar Arrhenius parameters are calculated for the addition of water to a thioaldehyde bonded to an sp² carbon.

Reactions 8 and 9 correspond to the addition of water to carbonyl sulfide, as investigated by Deng *et al.*,⁵² and transition state geometries for these reactions (as calculated in literature) are presented in Figure 4. Energies were recalculated in this study using CCSD(T)-F12a//VTZ-F12, and the barrier height is calculated to be 42 kJ/mol greater for the addition to the C=O bond than when water attacks the C=S bond. Comparing reaction 8 with the other hydration reactions with thiocarbonyl groups, we see that addition to carbonyl sulfide requires an activation energy more than 70 kJ/mol greater than reactions 1 through 4.

Because of the aromaticity of thiophene, addition reactions 10 and 11 are endothermic, in contrast to the exothermic addition of water to C-C double-bonds in alkenes. As such, these reactions proceed via much higher-energy pathways, and the parameters calculated in this study show that water will not appreciably react directly with thiophene at temperatures below 1500 K.

In each of the reactions where both single-point energy calculation methods were used, the addition reaction barrier height is calculated to be less using CCSD(T)-F12 than CBS-QB3, by an average of 4.5 kJ/mol. This is within the combined uncertainty of the two methods, but it suggests a systematic difference. Experimental data for this type of reactions will be quite useful for more substantial validation, but based on what we have seen so far in this and other works, we prefer the CCSD(T)-F12 calculations.

85 Molecular Addition of Hydrogen Sulfide

Reaction coefficients for eight reactions involving the addition of H₂S to a carbonyl bond, the reverse of which is the elimination of H₂S from a thiol, are presented in Table 5. The optimized transition states for reactions 14 and 19, addition of H₂S to propanal and carbon dioxide, respectively, were available in literature.^{9, 52} The other geometries were determined in this work and are reported in the Supporting Information. This type of reaction progresses in a similar fashion as the molecular addition of water to a thiocarbonyl compound. For this initial database, the bimolecular reaction was considered without an additional catalyst like water. As previous calculations have shown that water may catalyse this reaction in supercritical conditions,⁹ additional work in this area will be important to fully understanding this chemistry, and these calculations are currently being conducted. All of these reaction coefficients were calculated using CCSD(T)-F12a//VTZ-F12 energies, with the exception of reaction 17, for which the CBS-QB3 energies were used. CCSD(T)-F12 again predicts smaller barrier heights for each of these reactions, but by only an average of 2.2 kJ/mol for this reaction type.

This reaction occurs via a four-membered transition state, as in the addition of water to a double-bond, but the bond lengths and angles are greatly different. This is shown in Figure 5, which shows the optimized transition state for reaction 12, the addition of H₂S to formaldehyde. An IRC scan confirmed that this transition state corresponded to the expected reaction, and the potential energy surface was scanned using b3lyp/6-311G(2d,p), stepping the C—S and O—H bond distances while

optimizing the remaining variables. This is presented in Figure 6, and it shows that the reaction happens in a somewhat sequential fashion, with the translation of the hydrogen atom to form an OH group largely complete while the carbon and sulfur atoms are still separated by a distance of 2.7 Å (in comparison with the final C—S bond length of 1.8 Å). Thus, we expect that a separate disproportionation pathway exists with a similar transition state, although the addition reaction's transition state is over 100 kJ/mol more stable than the sum of the CH₂OH and SH radicals that would be the intermediates of a disproportion-recombination pathway. This reaction type is also a likely candidate for a roaming radical pathway, which has previously been investigated for the decomposition of formaldehyde.^{55, 56} In addition, investigating the possibility of reaction pathway bifurcation⁵⁷ may be an area of future research for this type of reaction system.

The carbon-sulfur distance in Figure 5 is calculated to be 46% greater in the transition state than the bond length in the product compound (compared to only a 12% difference for the carbon-oxygen distance in reaction 1). This is reflected in the general trend of activation energies, where the addition of water to a thioaldehyde is calculated to be a significantly more favorable reaction than the addition of H₂S to an aldehyde.

Similarly to the case with the addition of water to a thiocarbonyl compound, the reaction barrier in both directions is slightly lower when an alkyl group is substituted on the carbonyl compound, as shown by reactions 13 and 14 for addition to acetaldehyde and propanal, respectively. The transition states for these two reactions are presented in Figure 7. Again, this effect decreases as the chain length increases, so the calculated rate parameters for reaction 14 should be acceptable approximations for the addition of H₂S to a longer aldehyde. Substituting an alkyl group on both sides of the carbonyl group leads to slight steric hindrances, and a lower Arrhenius constant and greater n-factor is predicted for addition reaction 15.

Substitution of a phenyl group stabilizes the transition state of this reaction. In contrast to hydration reactions 5 and 6 which had very similar Arrhenius parameters, the energy barrier for the addition of H₂S to 2-propenal is calculated to be 6 kJ/mol lower than that calculated using CBS-QB3 for addition to benzaldehyde. However, the rate constants estimated using these parameters agree within a factor of two at temperatures above 600 K, and the disagreement will decrease at higher temperatures.

The optimized transition states of the addition of H₂S to acetic acid and carbon dioxide are presented in Figure 8. These are the only ones in Table 5 calculated to be endothermic in the addition direction, as these require addition to a stable carboxylic acid or carbon dioxide. The activation energies of these reactions are calculated to be the greatest of the reactions calculated in the addition direction, but the lowest in the H₂S elimination direction. These transition states have the shortest carbon-sulfur distance of any calculated for this type of reaction, and this length is 14% less for the addition of H₂S to CO₂ than for the addition to acetic acid.

Hydrogen Abstraction Reactions

Modified Arrhenius parameters for the 10 hydrogen abstraction reactions calculated in this work using CCSD(T)-F12a//VTZ-F12 energies are presented in Table 6.

Reactions 20-25 show the abstraction of hydrogen from a sulfur compound by an oxygen radical center. The first four reactions correspond to hydrogen transfer between hydrogen sulphide or methanethiol and hydroxyl or methoxy radical. These are favored in the forward direction, due to the much greater hydrogen-affinity of an oxygen atom relative to the sulfur atom. Linear transition states were found for most of these reactions, which is typical for hydrogen abstractions. However, linear and nonlinear transition states were found for hydrogen abstraction from H₂S by hydroxyl radical, and these are presented in Figure 9. IRC scans were conducted for the converged geometries, and they showed that both versions of each transition state corresponded to the correct reaction. Lower potential energies were calculated using the bent transition state, so this geometry was used to calculate rate parameters for this reaction.

The reaction between hydrogen sulphide and hydroxyl radical has previously been studied in experimental⁵⁸⁻⁶² and theoretical⁶³ investigations. The rate constants estimated in this work are compared with experimental data in Figure 10. Only the M06-X calculation approximated the experimentally observed temperature dependence (although with quite a bit of scatter, and hence uncertainty is observed in the experimental data) due to an addition complex below the reactants' total energy. Using our methods, the optimized prereactive complex had an energy approximately equal to the reactants, so our TST calculations do not capture the negative temperature dependence at very low temperatures (below 300 K, where rate parameters were not directly calculated for this study). However, all of the methods employed in this work come within about 20% of the experimental data at the temperatures relevant to combustion and pyrolysis, and slightly better agreement was obtained using the quadruple-zeta than the triple-zeta basis set.

For hydrogen abstraction from methanethiol by hydroxyl radical, a valid transition state was only found for the angled geometry. The energy of the transition state for this reaction was calculated to be 12.3 kJ/mol lower than the initial reactants, and a prereactive complex was optimized at an energy 19.4 kJ/mol lower than that of the reactants, which is illustrated in Figure 11. The estimated rate of this reaction approximately equals the collision rate at temperatures above 400 K, and this is reflected in the optimized effective rate parameters (the actual k_{eff} 's calculated are provided in the Supplementary Information).

Nearly linear transition state geometries were found for hydrogen abstraction from H₂S and methanethiol by vinyloxy radical (reactions 24 and 25, respectively), as both saddle point geometries had an O-H-S angle greater than 170°. Reaction 24 was the only one found to be exothermic in the direction of hydrogen abstraction from the hydroxyl group, while reaction 25 is isothermal (within the margin of error for the calculations). This is in agreement with published

thermochemistry data, from which standard enthalpies of reaction are estimated to be -18.2 and -4.3 kJ/mol for reactions 24 and 25, respectively.^{16, 64-67}

Reactions 26 and 27 represent the abstraction of an aldehydic hydrogen by a sulfur-containing radical (mercapto radical and 1-thioethyl radical, respectively). Low activation energies are calculated for reaction 26 in both directions, while abstraction of the hydrogen of the carbon adjacent to a thiol group is found to be significantly less favorable. However, this activation energy is 27 kJ/mol lower than that calculated for the abstraction of hydrogen from propane by acetyl radical to form isopropyl radical and acetaldehyde,⁶⁸ as the alpha radical in a thiol or sulfide is stabilized by the presence of sulfur. These two values are compared in Table 7.

Reactions 28-30 were calculated as possible intermediate steps in the desulfurization of alkyl sulfides and thiols in supercritical water. Reactions 28 and 29, hydrogen abstraction from a geminal mercaptoalcohol by a methyl or thiyl radical, show significantly lower activation energies than generally observed for the abstraction of a hydrogen from tetravalent carbon, as the resulting radical is stabilized by the neighboring sulfur and oxygen atoms. These reactions will be slightly sterically hindered by the neighboring groups, and this effect will increase in similar reactions with larger attacking species. Treatment of the coupling of hindered rotors will likely lead to more accurate rate predictions, so this should be considered when kinetic model predictions are particularly sensitive to this type of reaction.

Reaction 30, the abstraction of hydrogen from thioformic acid by a methyl radical, is highly exothermic, and the radical formed in this reaction is stabilized by the carbonyl group. A negative activation energy was fit to this reaction, but the ΔE_0 is positive and the positive relationship between temperature and rate constant is expressed by the n-factor of 3.5.

35 Radical Addition to Double Bonds (Reverse Beta-Scission)

Modified Arrhenius parameters for the seven radical addition reactions calculated in this work using CCSD(T)-F12a//VTZ-F12 energies are presented in Table 8. A mean absolute deviation of only 2.5 kJ/mol is calculated for the barrier height calculated using CCSD(T)-F12a versus CBS-QB3.

Optimized transition states for the addition reactions of radicals on thioformic acid are presented in Figure 12. The reverse of reaction 31, which forms thioformic acid and a hydrogen atom, is calculated to be significantly less favorable than the beta scission reactions (reverse of 32 and 33) that form the same thioformic acid and alkyl radicals. The transition state of reaction 34, addition of hydrogen to the sulfur atom of the C—S double-bond, is calculated to have a slightly negative activation energy and barrier height. The transition state for this reaction is presented in Figure 13, showing that the lowest energy conformer for this transition state corresponds to attack of hydrogen from the alcohol side of the other reactant. Interaction between the two hydrogen atoms leads to a slight decrease in the barrier height, and suggested that this was actually an H₂ insertion reaction. Additional scans were conducted to confirm that this was indeed a radical addition/beta-scission reaction.

Reverse reactions 35 and 36 form the stable carbonyl sulfide and either the hydrogen or methyl radical. These are calculated to be significantly less endothermic than reverse reactions 31-34; so as expected, much lower activation energies are calculated in the beta scission direction, while greater activation energies are predicted in the addition direction.

A significantly submerged reaction barrier was calculated for the addition of thiyl radical to 1-propenol, and a pre-reactive complex was optimized near the transition state geometry. The potential energy surface of this reaction is presented in Figure 14. The conversion of the pre-reactive complex to form the product is calculated to occur significantly faster than the reverse reaction to reform the reactants at temperatures greater than 400 K: thus, the overall k_{eff} is calculated to exhibit very little temperature dependence and remain approximately equal to the collision rate (additional details available in the Supplementary Information).

Tautomerization of Thiocarboxylic Acids

Three elementary tautomerization reactions were calculated in this work using CCSD(T)-F12a//VTZ-F12 energies, and they are shown in Table 9. These occur via the translation of a hydrogen atom from an alcohol group of a thiocarboxylic acid to the sulfur atom.

The three reactions calculated in Table 9 proceed via very similar transition states, as shown in Figure 15. Interatomic distances vary by less than 0.03 Å between the saddle point geometries for reactions 38 and 39 (tautomerization of thioformic and thioacetic acid, respectively), and the rate parameters calculated vary only slightly. The transition state is stabilized to some extent by the substitution of an alkyl group, but this only leads to a difference of 6 kJ/mol in the forward barrier height of reactions 39 and 40 in comparison with reaction 38. Reactions 39 and 40 are calculated to have nearly identical Arrhenius parameters, and Figure 15 shows that the relevant interatomic distances for these two reactions are nearly identical. We expect that further increasing of the alkyl chain length should have a negligible effect. Thus, the coefficients calculated for reaction 40, the tautomerization of thiopropionic acid, should be acceptable for elementary tautomerization reactions of thiocarboxylic acids containing alkyl chains.

Based on the rate coefficients calculated for the tautomerization of thiopropionic acid, a thiocarboxylic acid with a C=S bond would have a half-life of less than 0.1 s at temperatures above 500 K. It is recommended to include this pathway in any model where this type of compound is likely to be produced.

Thermochemical Library

Thermochemistry Group Additivity Values (GAV)⁶⁹ for the 15 groups calculated in this work using CBS-QB3 are presented in **Error! Reference source not found.**, and Hydrogen Bond Increments (HBI)⁴³ for the two radical groups are presented in **Error! Reference source not found.** Previous comparisons with a small set of sulfur compounds with experimental thermochemistry showed that these calculations are generally accurate within 4 kJ/mol.^{16, 38} These groups are primarily relevant to the SCW pyrolysis of sulfides and thiols; they

represent a small subset of all possible groups containing carbon, sulfur, and oxygen. Future expansion of this group library will be necessary for modeling more oxidized systems, for which more extensive experimental data are available for benchmarking.⁷⁰⁻⁷⁴ In addition, regression of BAC and GAV using CCSD(T)-F12 for organic compounds should provide more accurate estimates for thermochemical parameters, and these calculations are currently being conducted.

Standard heats of formation, entropies, and heat capacities between 300 and 2400 K were calculated using CBS-QB3 for each of the molecules involved in the reactions investigated in this work, as well as for some additional molecules for use as a training set in GAV regression. These are included in the supporting information as both a data table and a file of NASA polynomials.

Conclusions

Rate coefficients and thermochemical parameters were calculated for 40 reactions involving sulfur and oxygen compounds. These have applicability in studies of sulfur chemistry in an environment rich in water or other oxygenated species, such as the reactions of organosulfur compounds in supercritical water reactors or in geological formations where water is present.

Although the calculation methods employed in this work are among the most accurate available, rate coefficients calculated using these methods can still have greater than factor-of-2 uncertainty. In situations where more accurate rate parameters are required, experiments (if possible) or calculations using higher-level quantum chemistry methods and improved treatments of anharmonicity should be conducted.^{75, 76} The parameters calculated in this work provide a good starting point for the kinetic modeling of organosulfur chemistry in supercritical water.

Acknowledgements

Saudi Aramco is gratefully acknowledged for financial support (contract number 6600023444).

References

1. C. Song, *Catalysis Today*, 2003, **86**, 211-263.
2. D. T. Johnston, *Earth-Science Reviews*, 2011, **106**, 161-183.
3. M. D. Lewan, *Geochimica et Cosmochimica Acta*, 1997, **61**, 3691-3723.
4. M. D. Lewan, *Nature*, 1998, **391**, 164-166.
5. M. D. Lewan and S. Roy, *Organic Geochemistry*, 2011, **42**, 31-41.
6. EIA. Retrieved 03/19/2014 from http://www.eia.gov/dnav/pet/pet_pnp_crq_dcu_nus_m.htm.
7. L. A. Gonzalez, P. Kracke, W. H. Green, J. W. Tester, L. M. Shafer and M. T. Timko, *Energy & Fuels*, 2012, **26**, 5164-5176.
8. J. D. V. Hamme, A. Singh and O. P. Ward, *Microbiology and Molecular Biology Reviews*, 2003, **67**.
9. Y. Kida, C. A. Class, A. J. Concepcion, M. T. Timko and W. H. Green, *Phys Chem Chem Phys*, 2014, **16**, 9220-9228.
10. M. Morimoto, Y. Sugimoto, Y. Saotome, S. Sato and T. Takanohashi, *The Journal of Supercritical Fluids*, 2010, **55**, 223.
11. L.-Q. Zhao, Z.-M. Cheng, Y. Ding, P.-Q. Yuan, S.-X. Lu and W.-K. Yuan, *Energy & Fuels*, 2006, **20**, 2067.
12. A. R. Katritzky, R. A. Barcock, M. Balasubramanian and J. V. Greenhill, *Energy & Fuels*, 1993, **8**, 498-506.
13. N. J. Cooper, *Compr. Org. Funct. Group Transform. II*, 2005, **3**, 355-396.
14. A. G. Vandeputte, M. K. Sabbe, M.-F. Reyniers and G. B. Marin, *Phys Chem Chem Phys*, 2012, **14**, 12773-12793.
15. A. G. Vandeputte, University of Ghent, 2012.
16. A. G. Vandeputte, M. K. Sabbe, M.-F. Reyniers and G. B. Marin, *Chemistry-A European Journal*, 2011, **17**, 7656-7673.
17. K. J. Hughes, A. S. Tomlin, V. A. Dupont and M. Pourkashanian, *Faraday Discuss.*, 2001, **2001**, 337-352.
18. P. Glarborg, D. Kubel, K. Dam-Johansen, H. M. Chiang and J. W. Bozzelli, *International Journal of Chemical Kinetics*, 1996, **28**, 773-790.
19. M. J. Frisch, G. W. Trucks, H. B. Schlegel, G. E. Scuseria, M. A. Robb, J. R. Cheeseman, J. Montgomery, J. A., T. Vreven, K. N. Kudin, J. C. Burant, J. M. Millam, S. S. Iyengar, J. Tomasi, V. Barone, B. Mennucci, M. Cossi, G. Scalmani, N. Rega, G. A. Petersson, H. Nakatsuji, M. Hada, M. Ehara, K. Toyota, R. Fukuda, J. Hasegawa, M. Ishida, T. Nakajima, Y. Honda, O. Kitao, H. Nakai, M. Klene, X. Li, J. E. Knox, H. P. Hratchian, J. B. Cross, V. Bakken, C. Adamo, J. Jaramillo, R. Gomperts, R. E. Stratmann, O. Yazyev, A. J. Austin, R. Cammi, C. Pomelli, J. W. Ochterski, P. Y. Ayala, K. Morokuma, G. A. Voth, P. Salvador, J. J. Dannenberg, V. G. Zakrzewski, S. Dapprich, A. D. Daniels, M. C. Strain, O. Farkas, D. K. Malick, A. D. Rabuck, K. Raghavachari, J. B. Foresman, J. V. Ortiz, Q. Cui, A. G. Baboul, S. Clifford, J. Cioslowski, B. B. Stefanov, G. Liu, A. Liashenko, P. Piskorz, I. Komaromi, R. L. Martin, D. J. Fox, T. Keith, M. A. Al-Laham, C. Y. Peng, A. Nanayakkara, M. Challacombe, P. M. W. Gill, B. Johnson, W. Chen, M. W. Wong, C. Gonzalez and J. A. Pople, *Gaussian 03*, (2004) Gaussian, Inc., Wallingford CT.
20. H.-J. Werner, P. J. Knowles, G. Knizia, F. R. Manby and M. Schütz, *Molpro: a general-purpose quantum chemistry program package*. In *Wiley Interdisciplinary Reviews: Computational Molecular Science*, 2011, **2**, 242-253.
21. A. D. Becke, *Journal of Chemical Physics*, 1992, **98**, 5648-5652.
22. J. A. Montgomery Jr., M. J. Frisch, J. W. Ochterski and G. A. Petersson, *Journal of Chemical Physics*, 1998, **110**, 2822-2827.
23. J. A. Montgomery Jr., M. J. Frisch, J. W. Ochterski and G. A. Petersson, *Journal of Chemical Physics*, 2000, **112**, 6532-6542.
24. T. B. Adler, G. Knizia and H.-J. Werner, *Journal of Chemical Physics*, 2007, **127**, 221106.
25. T. B. Adler, H.-J. Werner and F. R. Manby, *Journal of Chemical Physics*, 2009, **130**, 054106.
26. G. Knizia, T. B. Adler and H.-J. Werner, *Journal of Chemical Physics*, 2009, **130**, 054104.
27. K. A. Peterson, T. B. Adler and H.-J. Werner, *Journal of Chemical Physics*, 2008, **128**, 084102.
28. R. J. Bartlett and M. Musial, *Reviews of Modern Physics*, 2007, **79**, 291-352.

29. K. Raghavachari, G. W. Trucks, J. A. Pople and M. Head-Gordon, *Chemical Physics Letters*, 1989, **157**, 479-483.
30. J. D. Watts, J. Gauss and R. J. Bartlett, *Journal of Chemical Physics*, 1993, **98**, 8718-8733.
- 5 31. J. M. L. Martin, *Chemical Physics Letters*, 1996, **259**, 669-678.
32. J. Aguilera-Iparraguirre, A. D. Boese, W. Klopper and B. Ruscic, *Chemical Physics*, 2008, **346**, 56-68.
33. J. Aguilera-Iparraguirre, H. J. Curran, W. Klopper and J. M. Simmie, *Journal of Physical Chemistry A*, 2008, **112**, 7047-7054.
- 10 34. W. Klopper, R. A. Bachorz, D. P. Tew, J. Aguilera-Iparraguirre, Y. Carissan and C. Hättig, *Journal of Physical Chemistry A*, 2009, **113**, 11679-11684.
35. W. Klopper and J. Noga, in *Chemistry and Physics*, ed. J. Rychlewski, Dordrecht, 2003.
- 15 36. J. Noga and W. Kutzelnigg, *Journal of Chemical Physics*, 1994, **101**, 7738-7762.
37. J. Zheng, Y. Zhao and D. G. Truhlar, *J. Chem. Theory Comput.*, 2009, **5**, 808-821.
38. A. G. Vandeputte, M.-F. Reyniers and G. B. Marin, *Theor Chem Account*, 2009, **123**, 391-412.
- 20 39. G. A. Petersson, D. K. Malick, W. G. Wilson, J. W. Ochterski, J. A. Montgomery and M. J. Frisch, *Journal of Chemical Physics*, 1998, **109**, 10570-10579.
40. Y. Zhao and D. G. Truhlar, *Accounts of Chemical Research*, 2008, **41**, 157-167.
- 25 41. A. D. Boese and J. M. L. Martin, *Journal of Chemical Physics*, 2004, **121**, 3405-3416.
42. S. Sharma, M. R. Harper and W. H. Green, *CanTherm open-source software package*, Massachusetts Institute of Technology, Cambridge, MA, 2010.
- 30 43. T. H. Lay, J. W. Bozzelli, A. M. Dean and E. R. Ritter, *J. Phys. Chem.*, 1995, **99**, 14514-14527.
44. H. S. Johnston and J. Heicklen, *Journal of Physical Chemistry*, 1962, **66**, 532-533.
- 35 45. C. Eckart, *Physical Review*, 1930, **35**, 1303-1309.
46. J. Pen, X. Hu and P. Marshall, *J. Phys. Chem. A*, 1999, **103**, 5307-5311.
47. H. Arican and N. L. Arthur, *Aust. J. Chem.*, 1983, **36**, 2195-2202.
48. L. G. S. Shum and S. W. Benson, *Int. J. Chem. Kinet.*, 1985, **17**, 749-761.
- 40 49. N. M. Marinov, *Int. J. Chem. Kinet.*, 1999, **31**, 1999.
50. F. A. Bischoff, S. Wolfsegger and D. P. Tew, *Molecular Physics*, 2009, **107**, 963-975.
51. A. Jalan, I. M. Alecu, R. Meana-Pañeda, J. Aguilera-Iparraguirre, K. R. Yang, S. S. Merchant, D. G. Truhlar and W. H. Green, *J. Am. Chem. Soc.*, 2013, **135**, 11100-11114.
- 45 52. C. Deng, Q.-G. Li, Y. Ren, N.-B. Wong, S.-Y. Chu and H.-J. Zhu, *Journal of Computational Chemistry*, 2007, **29**, 466-480.
53. J. Li, A. Kazakov and F. L. Dryer, *J. Phys. Chem. A*, 2004, **108**, 7671-7680.
- 50 54. D. R. Kent, S. L. Widicus, G. A. Blake and W. A. Goddard, *Journal of Chemical Physics*, 2003, **119**, 5117-5120.
55. L. B. Harding, Y. Georgievskii and S. J. Klippenstein, *J. Phys. Chem. A*, 2010, **114**, 765-777.
- 55 56. L. B. Harding and S. J. Klippenstein, *J. Phys. Chem. Lett.*, 2010, **1**, 3016-3020.
57. D. H. Ess, S. E. Wheeler, R. G. Iafe, L. Xu, N. Çelebi-Ölçüm and K. N. Houk, *Angew. Chem. Int. Ed.*, 2008, **47**, 7592-7601.
58. C. Lafage, J.-F. Pauwels, M. Carlier and P. Devolder, *J. Chem. Soc. Faraday Trans. 2*, 1987, **83**, 731-739.
- 60 59. J. V. Michael, D. F. Nava, W. D. Brobst, R. P. Borkowski and L. J. Stief, *J. Phys. Chem.*, 1982, **86**, 81-84.
60. R. A. Perry, R. Atkinson and J. N. Pitts Jr., *J. Chem. Phys.*, 1976, **64**, 3237-3239.
- 65 61. G. S. Tyndall and A. R. Ravishankara, *International Journal of Chemical Kinetics*, 1991, **23**, 483-527.
62. A. A. Westenberg and N. deHaas, *J. Chem. Phys.*, 1973, **59**, 6685-6686.
63. B. A. Ellingson and D. G. Truhlar, *J. Am. Chem. Soc.*, 2007, **129**, 12765-12771.
- 70 64. M. W. Chase, Jr., *J. Phys. Chem. Ref. Data*, 1998, **Monograph 9**, 1-1951.
65. G. da Silva, C.-H. Kim and J. W. Bozzelli, *J. Phys. Chem. A*, 2006, **110**, 7925-7934.
- 75 66. D. P. Tabor, M. E. Harding, T. Ichino and J. F. Stanton, *J. Phys. Chem. A*, 2012, **116**, 7668-7676.
67. W. D. Good, J. L. Lacina and J. P. McCullough, *J. Phys. Chem.*, 1961, **65**, 2229-2231.
68. W. Tsang, *Journal of Physical and Chemical Reference Data*, 1988, **17**, 887-952.
- 80 69. S. W. Benson and J. H. Buss, *Journal of Chemical Physics*, 1958, **29**, 546-572.
70. F. Turecek, L. Brabec, T. Vondrak, V. Hanus, J. Hajicek and Z. Havlas, *Collect. Czech. Chem. Commun.*, 1988, **53**, 2140-2158.
- 85 71. W. K. Busfield, H. Mackle and P. A. G. O'Hare, *Trans. Faraday Soc.*, 1961, **57**, 1054-1057.
72. H. Mackle and D. V. McNally, *Trans. Faraday Soc.*, 1969, **65**, 1738-1741.
73. H. Mackle and P. A. G. O'Hare, *Trans. Faraday Soc.*, 1961, **57**, 1070-1074.
- 90 74. H. Mackle and W. V. Steele, *Trans. Faraday Soc.*, 1969, **65**, 2053-2059.
75. B. C. Garrett and D. G. Truhlar, *Journal of Physical Chemistry*, 1979, **83**, 1915-1924.
- 95 76. J. Zheng, T. Yu, E. Papajak, I. M. Alecu, S. L. Mielke and D. G. Truhlar, *Phys Chem Chem Phys*, 2011, **13**, 10885-10907.

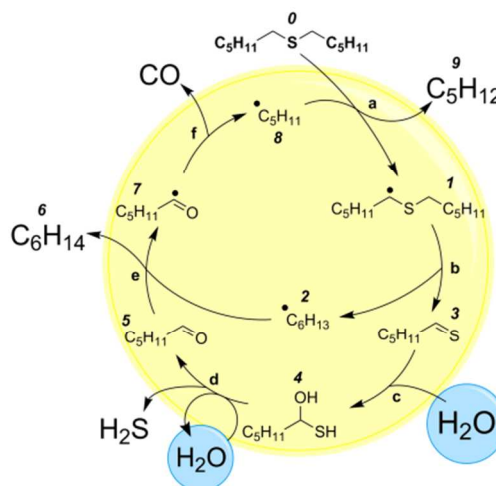


Figure 1. Proposed mechanism⁹ for conversion of hexyl sulfide to pentane and CO₂

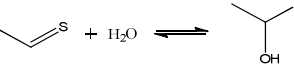
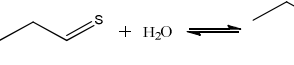
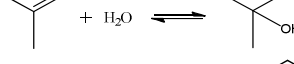
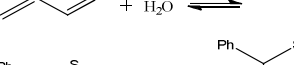
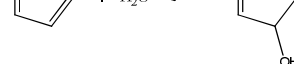
Table 1. Comparison of CBS-QB3 and CCSD(T)-F12 calculations with published data. Published value for reaction *c* was theoretically estimated. *T* (K), *k_f* [cm³/(mol*s) for bimolecular reactions, s⁻¹ for unimolecular reaction]

Reaction	Reference	<i>T</i>	<i>k_f(T)</i>				
			Published	CBS-QB3	VDZ-F12	VTZ-F12	VQZ-F12
a. $\text{H}_2\text{S} + \dot{\text{H}} \longrightarrow \text{H}_2 + \dot{\text{S}}\text{H}$	Pen [46]	400	1.4×10^6	2.0×10^6	2.2×10^6	2.5×10^6	2.3×10^6
b. $\text{H}_2\text{S} + \dot{\text{C}}\text{H}_3 \longrightarrow \text{CH}_4 + \dot{\text{S}}\text{H}$	Arican [47]	400	8.8×10^3	1.6×10^4	9.3×10^3	9.4×10^3	8.1×10^3
c. $\text{H}_2\text{C}=\text{S} + \dot{\text{C}}\text{H}_3 \longrightarrow \text{C}_6\text{H}_{11}\text{S}\cdot$	Shum [48]	700	9.4×10^4	9.3×10^5	4.3×10^5	4.7×10^5	4.6×10^5
d. $\text{C}_6\text{H}_{11}\text{OH} \longrightarrow \text{C}_2\text{H}_4 + \text{H}_2\text{O}$	Marinov [49]	500 700	5.8×10^{-16} 1.1×10^{-7}	9.8×10^{-17} 1.4×10^{-8}	7.3×10^{-16} 6.0×10^{-8}	5.6×10^{-16} 5.0×10^{-8}	4.2×10^{-16} 4.1×10^{-8}

Table 2. Mean absolute difference in barrier height (kJ/mol) calculated using double-, triple-, and quadruple-zeta basis sets with CCSD(T)-F12a.

	Reaction #				Average
	1	12	20	31	
DZ-QZ	1.21	0.31	1.57	1.67	1.19
TZ-QZ	0.01	0.57	0.34	0.16	0.27

Table 3. Modified Arrhenius coefficients for the molecular addition of water to sulfur-containing compounds. A [$\text{cm}^3/(\text{mol}\cdot\text{s})$ forward, s^{-1} reverse], n (unitless), E_a , ΔE_o , and $\Delta H^\circ_{\text{rxn}}$ (kJ/mol). Parameters for reaction 6 computed using CCSD(T)//B3LYP, the rest computed using CCSD(T)-F12a//VTZ-F12//B3LYP/CBSB7. $\Delta E_{o,F12}$ calculated using CCSD(T)-F12a//VTZ-F12, $\Delta E_{o,CBS}$ calculated using CBS-QB3.

Reaction	T	Forward Rate Parameters							Reverse Rate Parameters		
		$\log_{10}A$	n	E_a	$\Delta E_{o,F12}$	$\Delta E_{o,CBS}$	$\Delta H^\circ_{\text{rxn}}$	$\log_{10}A$	n	E_a	
1. 	300-2000	-0.62	3.55	101.8	122.7	127.6	-54.1	8.74	1.07	163.9	
2. 	300-2000	-2.42	3.96	102.7	123.5	127.2	-48.1	8.57	1.12	157.9	
3. 	300-2000	-2.58	3.95	101.3	121.6	125.3	-46.7	8.94	1.03	154.6	
4. 	300-2000	-4.30	4.54	101.7	125.0	125.9	-46.9	8.32	1.19	154.6	
5. 	300-2000	-1.22	3.75	122.8	140.9	145.6	-28.4	8.01	1.32	157.0	
6. 	300-2000	-1.78	3.90	123.1	n.c.	144.3	-29.6	7.75	1.44	158.5	
7. 	400-2000	-2.32	3.87	141.3	160.2	163.7	-8.3	4.92	1.98	150.4	
8. 	500-2000	0.20	3.50	172.9	187.8	193.9	13.8	11.87	0.33	171.2	
9. 	500-2000	-0.66	3.70	209.9	230.4	235.4	35.6	11.91	0.38	182.9	
10. 	600-2000	-2.8	4.32	244.7	269.3	274.7	33.9	7.59	1.79	215.2	
11. 	500-2000	-1.6	4.13	244.0	264.4	271.2	37.0	8.60	1.63	210.4	

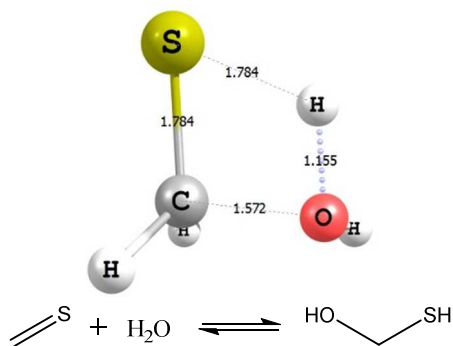


Figure 2. Optimized transition state for the hydration of thioformaldehyde. Distances (Ångstroms).

Table 4. Reaction barriers (kJ/mol) for hydration of thioformaldehyde, formaldehyde, and ethene. Data for the first reaction calculated using CCSD(T)-F12.

Reaction	$\Delta E_{o,f}$	$\Delta E_{o,r}$	Ref.
$\text{H}_2\text{C}=\text{S} + \text{H}_2\text{O} \rightleftharpoons \text{HO}-\text{CH}_2-\text{SH}$	123	173	this work
$\text{H}_2\text{C}=\text{O} + \text{H}_2\text{O} \rightleftharpoons \text{HO}-\text{CH}_2-\text{OH}$	166	189	Kent [54]
$\text{H}_2\text{C}=\text{CH}_2 + \text{H}_2\text{O} \rightleftharpoons \text{HO}-\text{CH}_2-\text{CH}_3$	209	254	Li [53]

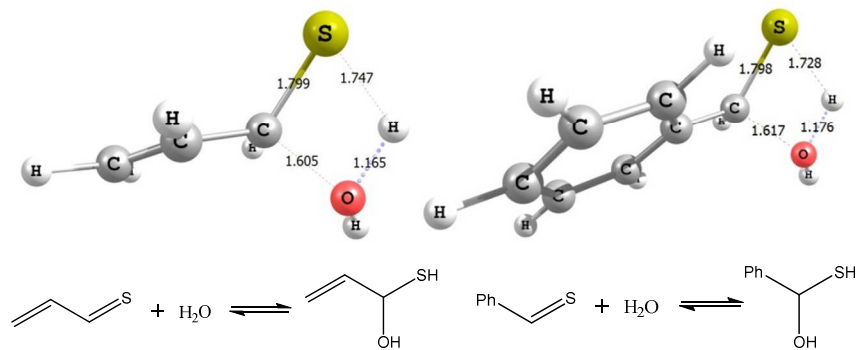


Figure 3. Transition states for the hydration of 2-propenethial (left) and benzenethial (right). Distances (Ångstroms).

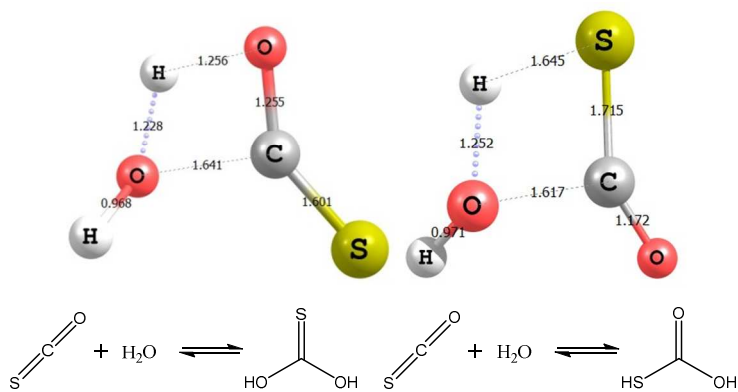
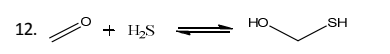
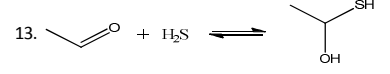
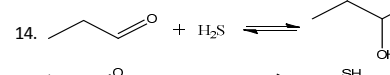
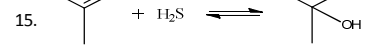
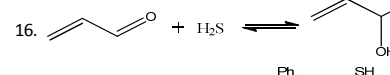
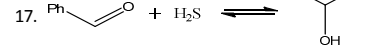
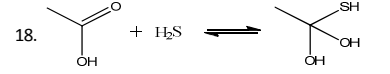
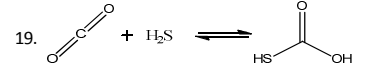


Figure 4. Transition states⁵² for the hydration of carbonyl (left) and thiocarbonyl (right) group of carbonyl sulfide. Distances (Ångstroms).

Table 5. Modified Arrhenius coefficients for the molecular addition of hydrogen sulfide to carbonyl compounds. A [$\text{cm}^3/(\text{mol}\cdot\text{s})$ forward, s^{-1} reverse], n (unitless), E_a , ΔE_o , and $\Delta H^\circ_{\text{rxn}}$ (kJ/mol). Parameters for reaction 17 computed using CCSD(T)//B3LYP, the rest computed using CCSD(T)-F12a//VTZ-F12 energies. $\Delta E_{o,F12}$ calculated using CCSD(T)-F12a//VTZ-F12, $\Delta E_{o,CBS}$ calculated using CBS-QB3.

Reaction	T	Forward Rate Parameters						Reverse Rate Parameters		
		$\log_{10}A$	n	E_a	$\Delta E_{o,F12}$	$\Delta E_{o,CBS}$	$\Delta H^\circ_{\text{rxn}}$	$\log_{10}A$	n	E_a
12. 	300-2000	1.09	3.27	156.7	170.0	172.7	-50.1	10.5	0.82	209.9
13. 	300-2000	1.78	2.93	153.5	161.8	164.4	-34.1	12.9	0.13	189.5
14. 	300-2000	1.49	2.96	152.0	159.9	162.8	-32.9	13.4	0.01	187.3
15. 	300-2000	0.22	3.45	158.0	168.7	169.1	-26.1	13.0	0.16	184.0
16. 	300-2000	2.58	2.72	151.8	159.1	159.2	-22.0	12.5	0.20	177.3
17. 	300-2000	2.09	2.83	145.1	n.c.	153.0	-20.5	11.6	0.45	169.9
18. 	300-2000	-0.68	3.60	159.7	170.4	171.8	31.9	7.04	1.65	120.6
19. 	500-2000	0.71	3.52	190.2	204.0	209.4	40.7	11.44	0.59	154.8

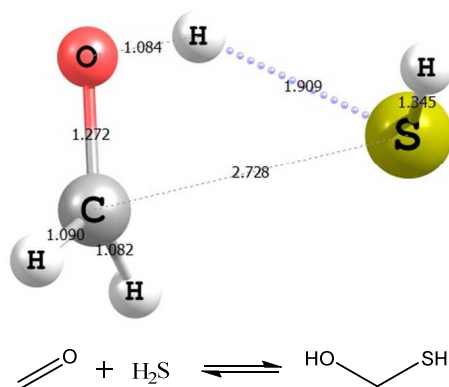


Figure 5. Transition state for the molecular addition of H_2S to formaldehyde. Distances (Ångstroms).

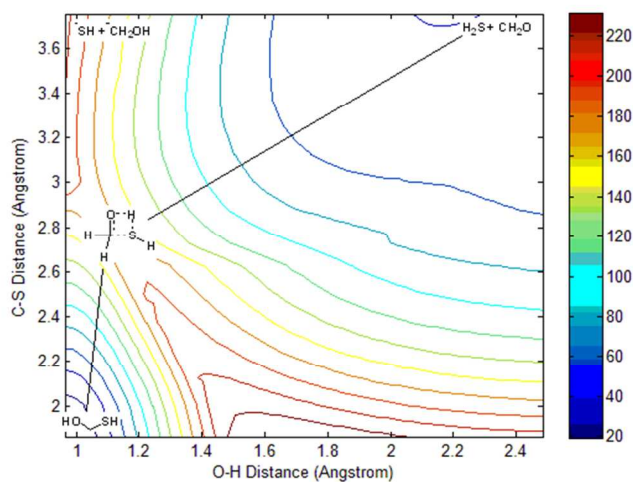


Figure 6. Potential energy surface for H_2S addition reaction 12. Energies (kJ/mol) relative to the mercaptoalcohol.

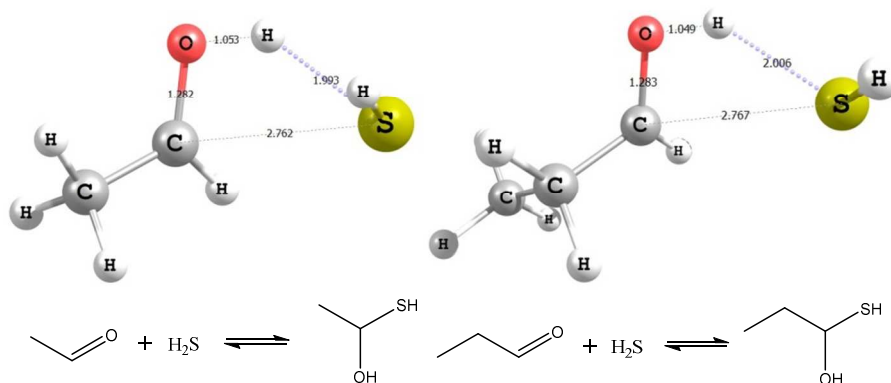


Figure 7. Transition states for the molecular addition of H_2S to acetaldehyde (left) and propanal (right). Distances (Ångstroms).

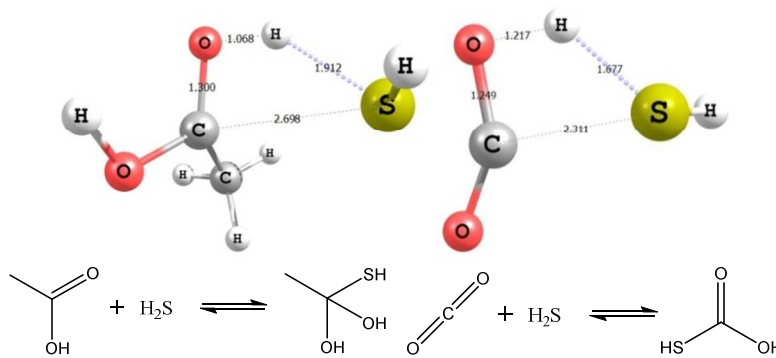
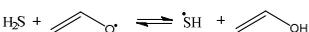
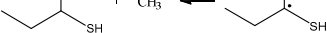
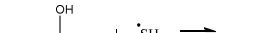


Figure 8. Transition states for the endothermic addition of H_2S to acetic acid (left) and carbon dioxide (right). Distances (Ångstroms).

Table 6. Modified Arrhenius coefficients for hydrogen abstraction reactions. Reaction 21 estimated for overall pathway including pre-reactive complex at high-pressure limit. A [cm³/(mol*s)], n (unitless), Ea, ΔEo, and ΔH°_{rxn} (kJ/mol). Parameters computed using CCSD(T)-F12a//VTZ-F12//B3LYP/CBSB7. ΔEo_{F12} calculated using CCSD(T)-F12a//VTZ-F12//B3LYP/CBSB7, ΔEo_{CBS} calculated using CBS-QB3.

Reaction	T	Forward Rate Parameters						Reverse Rate Parameters		
		log ₁₀ A	n	E _a	ΔE _{o,F12}	ΔE _{o,CBS}	ΔH° _{rxn}	log ₁₀ A	n	E _a
20. H ₂ S + •OH ⇌ •SH + H ₂ O	300-2000	7.80	1.71	-2.8	4.4	3.1	-114.1	7.08	2.00	109.60
21. 	300-2000	13.0	0.03	1.9	-12.3	-3.2	-136.7	2.22	3.56	114.86
22. H ₂ S + 	300-2000	4.32	2.44	5.0	14.9	20.7	-56.3	2.99	2.92	59.78
23. 	300-2000	6.12	2.09	-2.0	-1.0	13.6	-78.9	2.41	3.43	72.47
24. H ₂ S + 	500-2000	1.71	3.34	63.6	77.0	81.1	22.5	2.53	3.21	37.54
25. 	500-2000	1.65	3.28	68.4	79.4	78.9	-0.10	-0.06	4.06	61.62
26. 	300-2000	4.08	2.90	0.74	6.8	2.2	-9.8	2.63	3.07	10.07
27. 	500-2000	0.26	3.63	35.2	44.9	39.4	-19.4	0.11	3.78	53.90
28. 	400-2000	1.03	3.44	17.9	35.2	31.3	-55.2	0.29	3.81	74.34
29. 	300-2000	5.04	2.47	3.1	18.1	4.6	-0.17	3.91	2.60	3.64
30. 	300-2000	0.13	3.51	-3.6	4.9	5.2	-59.3	-2.34	4.58	54.41

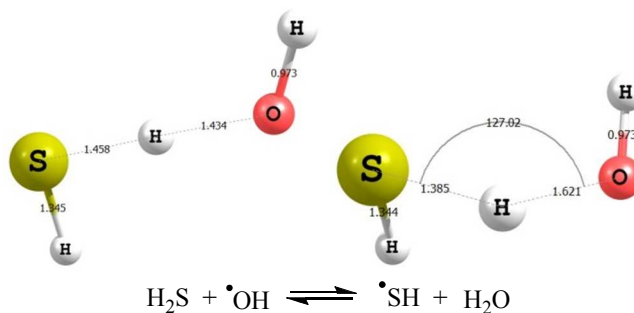


Figure 9. Linear (left) and angled (right) transition states optimized for hydrogen abstraction from hydrogen sulfide by the hydroxyl radical. Distances (Ångstroms) and angle (degrees).

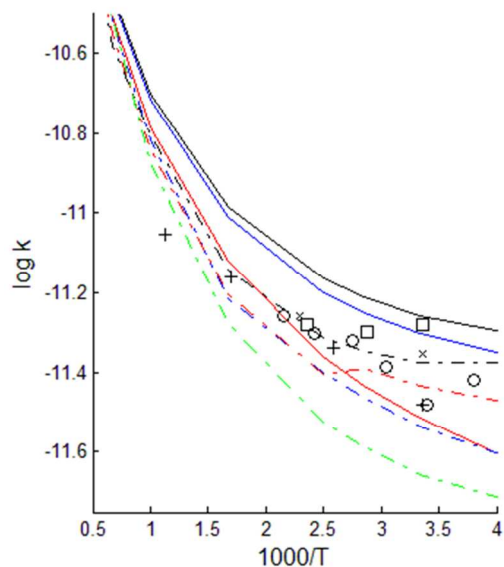


Figure 10. Comparison of rate coefficient calculations ($\text{cm}^3/\text{molecules/s}$) with experimental data for $\text{H}_2\text{S} + \text{OH} = \text{SH} + \text{H}_2\text{O}$. Lafage (o), Michael (x), Perry (\square), Westenberg (+), Ellingson (hashed): M06-2X (black), MPWB1K (blue), MPW1K (green), BB1K (red), This Work (solid): CBS-QB3 (red), CCSD(T)-F12a/VTZ-F12 (black), CCSD(T)-F12a/VQZ-F12 (blue)

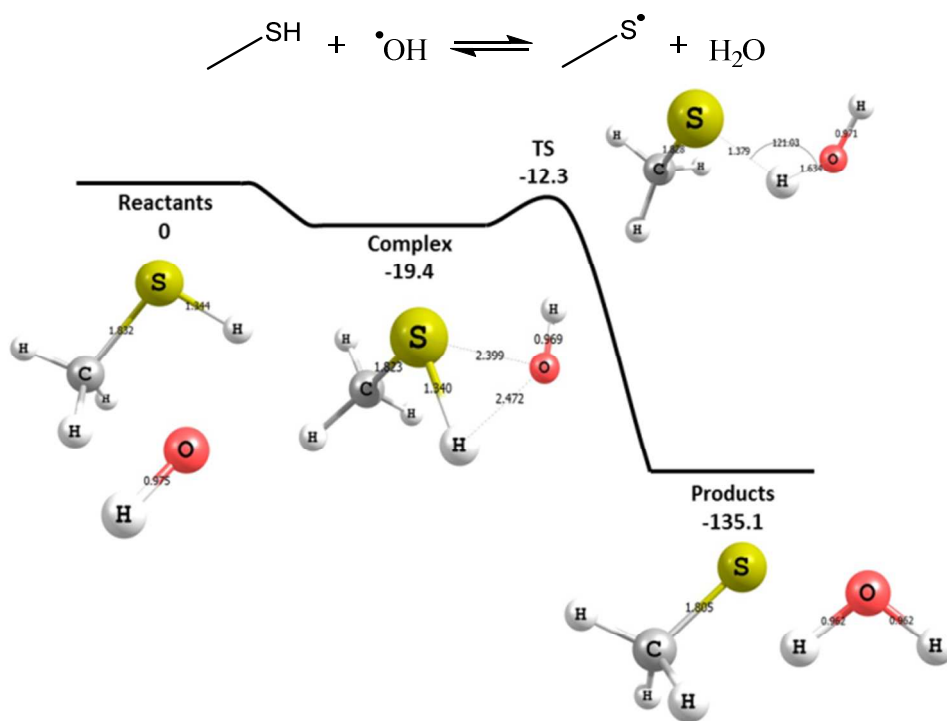


Figure 11. Potential energy surface for hydrogen abstraction from methanethiol by hydroxyl radical. Energies (kJ/mol), distances (\AA), angles (degrees). Note the submerged TS (saddle point energy less than energy of reactants).

Table 7. Forward reaction barriers (kJ/mol) for hydrogen abstraction reactions by the acetyl radical.

Reaction	ΔE_0	Ref.
	44.9	this work
	67.9	Tsang [68]

Table 8. Modified Arrhenius coefficients for radical addition to double bonds. Reaction 37 estimated for overall pathway including pre-reactive complex at high-pressure limit. A [$\text{cm}^3/(\text{mol}\cdot\text{s})$] forward, s^{-1} reverse], n (unitless), E_a , ΔE_0 , and $\Delta H^\circ_{\text{rxn}}$ (kJ/mol). Parameters computed using CCSD(T)-F12a//VTZ-F12 energies. $\Delta E_{0,\text{F12}}$ calculated using CCSD(T)-F12a//VTZ-F12, $\Delta E_{0,\text{CBS}}$ calculated using CBS-QB3.

Reaction	T	Forward Rate Parameters						Reverse Rate Parameters		
		$\log_{10} A$	n	E_a	$\Delta E_{0,\text{F12}}$	$\Delta E_{0,\text{CBS}}$	$\Delta H^\circ_{\text{rxn}}$	$\log_{10} A$	n	E_a
31.	300-2000	8.45	1.63	11.4	16.0	15.9	-132.1	7.83	1.83	143.4
32.	300-2000	4.36	2.35	23.0	28.5	29.4	-99.3	10.98	0.99	123.3
33.	300-2000	3.22	2.54	16.3	20.7	19.0	-96.0	12.35	0.55	112.8
34.	300-2000	9.30	1.21	-5.3	-0.41	3.3	-101.2	10.86	0.46	98.6
35.	300-2000	9.92	1.23	32.2	38.4	39.7	-38.8	9.03	1.33	73.7
36.	300-2000	6.91	1.68	54.2	59.1	56.3	-28.3	11.86	0.59	84.6
37.	300-2000	13.08	0.00	1.7	-9.3	-16.2	-41.6	12.61	0.14	24.6

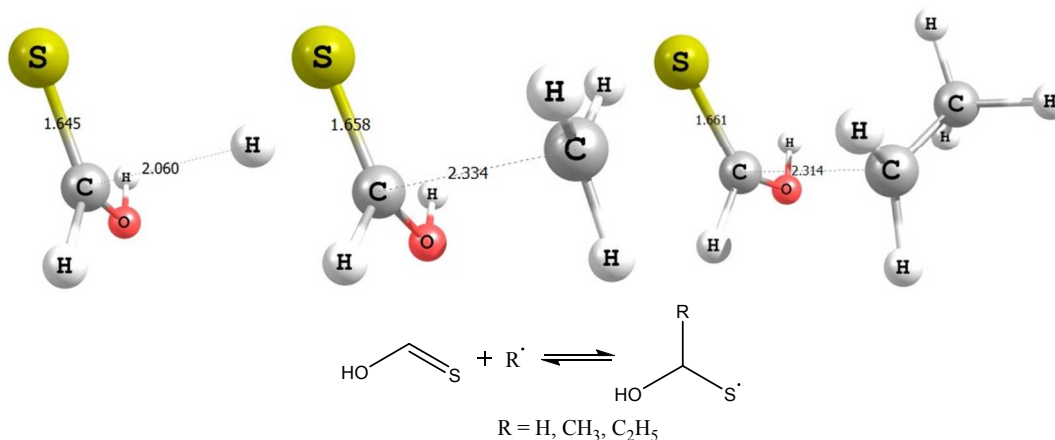


Figure 12. Transition states for radical additions to C=S bonds: reactions 31 (left), 32 (middle), and 33 (right). Distances (Ångstroms).

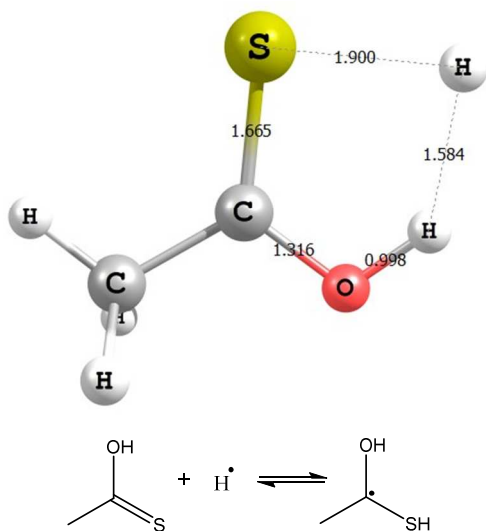


Figure 13. Transition state for radical addition to the S atom in thioacetic acid (reaction 34). Distances (Ångstroms).

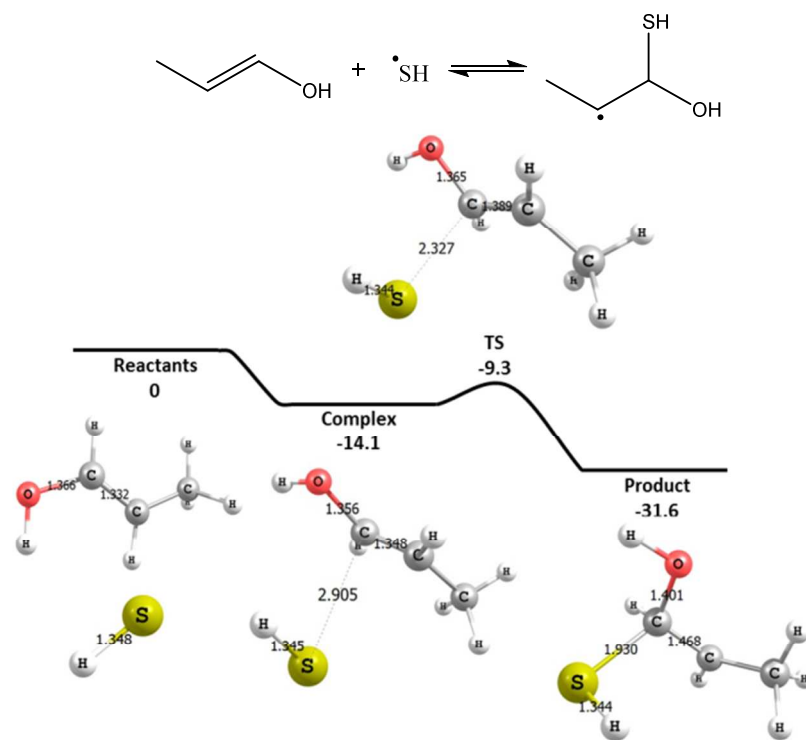


Figure 14. Potential energy surface for addition of thiol radical to carbon-1 in 1-propen-1-ol. Energies (kJ/mol), distances (Ångstroms). Note this reaction has a submerged TS, i.e. saddle point energy is lower than energy of reactants.

Table 9. Modified Arrhenius coefficients for elementary tautomerization reactions that include sulfur and oxygen. A (s^{-1}), n (unitless), E_a , ΔE_o , and ΔH°_{rxn} (kJ/mol). Parameters computed using CCSD(T)-F12a/VTZ-F12 energies. $\Delta E_{o,F12}$ calculated using CCSD(T)-F12a/VTZ-F12, $\Delta E_{o,CBS}$ calculated using CBS-QB3.

Reaction	T	Forward Rate Parameters							Reverse Rate Parameters		
		$\log_{10} A$	n	E_a	$\Delta E_{o,F12}$	$\Delta E_{o,CBS}$	ΔH°_{rxn}	$\log_{10} A$	n	E_a	
38.	300-2000	1.50	3.33	86.6	112.2	121.0	-8.6	1.12	3.25	96.8	
39.	300-2000	1.79	3.26	81.7	106.2	115.7	-9.9	1.64	3.09	95.5	
40.	300-2000	1.77	3.27	82.0	107.1	115.6	-8.6	1.85	3.05	94.4	

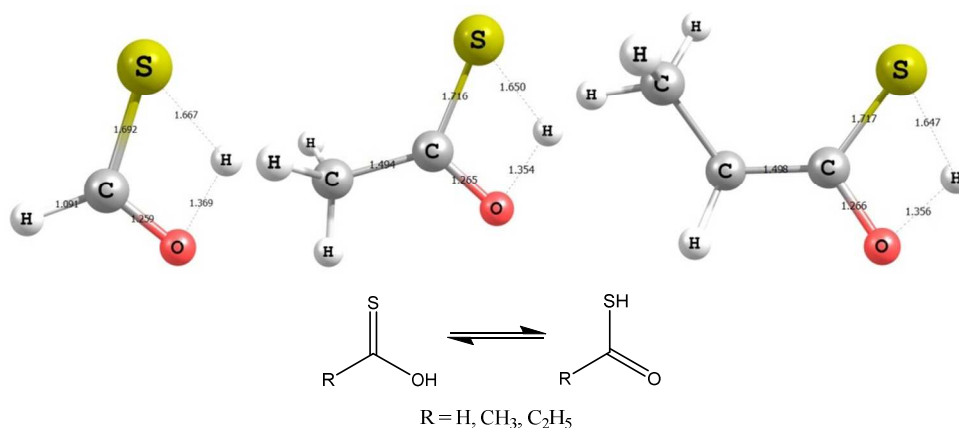


Figure 15. Transition states for tautomerization reactions 38 (left), 39 (middle), and 40 (right). Distances (Ångstroms).

Table 10. GAV for groups containing carbon, sulfur, and oxygen, based on CBS-QB3 calculations available in the Supplementary Material. Groups presented in Benson notation ⁶⁹. $\Delta_f H^\circ$ (kJ/mol), S°_{int} (J/mol/K) C_p° (J/mol/K)

Group	$\Delta_f H^\circ$	S°_{int}	Benson Group Additivity Values						
			C_p°						
			298 K	298 K	300 K	400 K	500 K	600 K	800 K
1. C-(O)(S)(H) ₂	-48.47	19.17	31.30	39.92	46.03	49.85	53.77	56.65	62.45
2. C-(C)(O)(S)(H)	-46.45	-67.54	35.04	43.19	46.44	47.28	47.28	46.90	48.55
3. C-(C) ₂ (O)(S)	-47.10	-166.24	34.12	42.46	44.72	44.02	40.76	37.69	34.90
4. C-(O) ₂ (S)(H)	-82.52	-55.49	26.61	36.47	42.37	45.52	48.36	49.85	52.41
5. C-(C)(O) ₂ (S)	-89.59	-153.57	27.84	35.28	38.63	39.64	39.44	38.48	37.17
6. CO-(S)(H)	-41.18	122.84	23.04	25.77	28.04	30.01	33.71	36.79	41.14
7. CO-(C)(S)	-58.64	35.77	18.29	21.09	23.04	24.38	26.32	27.10	26.70
8. CO-(O)(S)	-48.22	40.19	20.68	23.57	26.55	29.24	31.74	32.47	34.23
9. CS-(O)(H)	11.93	126.10	18.76	22.17	25.50	28.55	33.70	37.63	43.40
10. CS-(C)(O)	-5.54	36.08	16.31	17.46	19.24	21.35	25.44	28.27	31.14
11. CS-(O) ₂	-95.08	11.15	12.89	15.03	16.30	16.88	16.68	15.69	13.53
12. O-(CS)(H)	-131.29	134.20	29.22	34.92	39.68	43.43	48.47	51.30	54.35
13. O-(CS)(C)	-60.84	41.92	23.26	26.40	29.30	31.86	35.66	37.63	38.87
14. S-(CO)(H)	-88.10	148.14	33.66	38.09	41.65	44.55	48.63	51.30	55.46
15. S-(CO)(C)	-64.13	46.48	24.17	28.16	31.80	34.89	38.96	40.88	42.44

Table 11. HBI for radical groups containing carbon, sulfur, and oxygen, based on CBS-QB3 calculations available in the Supplementary Material. $\Delta_f H^\circ$ (kJ/mol), S°_{int} (J/mol/K) C_p° (J/mol/K)

Group	$\Delta_f H^\circ$	S°_{int}	Hydrogen atom bond increment						
			C_p°						
			298 K	298 K	300 K	400 K	500 K	600 K	800 K
16. C•-(C)(O)(S)	385.35	34.14	-24.14	-23.10	-20.84	-19.96	-24.35	-33.97	-59.54
17. S•-(CO)	375.97	-5.27	-40.79	-49.37	-56.02	-62.13	-72.84	-80.71	-89.62